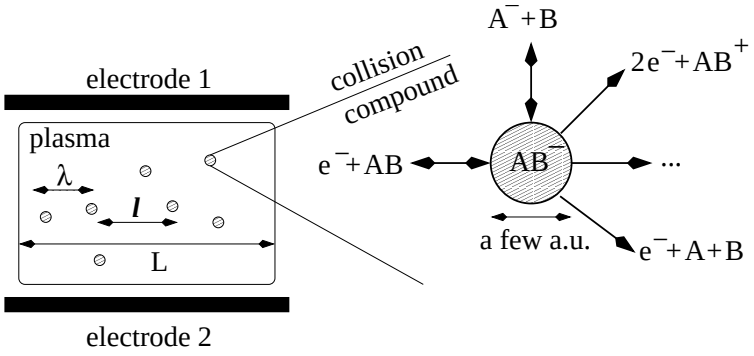

Figure 9.1: Schematic representation of the length scales in the bulk of a typical low-temperature gas discharge ($n_e = n_i = 10^{10}\ cm^{-3}$, $T_e = 10\ eV$, $T_i = 0.03\ eV$, and $n_{\rm gas} = 10^{16}\ cm^{-3}$). The macroscopic scales on which the Boltzmann-Poisson system operates are the spatial extension of the plasma $L \sim \mathcal{O}(cm)$, the mean-free-path of the species $l \sim \mathcal{O}(10^{-2}\ cm)$, and the plasma screening length $\lambda \sim \mathcal{O}(10^{-3}\ cm)$. On the rhs is an illustration of how the (temporary) collision compound AB^-, whose length scale is a few atomic units, that is, of the order of $10^{-7} cm$, controls the first six reactions of Table 9.1. The branching of the AB^- state at a given energy determines the cross sections for the reactions. The double arrow indicates that the fragments can appear in the entrance and the exit channel of a collision.

9.2 Elementary volume processes in gas discharges

Franz X. Bronold and Holger Fehske, Institut für Physik, Ernst-Moritz-Arndt-Universität Greifswald, Felix-Hausdorff-Str. 6, D–17489 Greifswald, Germany
(bronold(fehske)@physik.uni-greifswald.de)

The plasma chemistry of reactive gas discharges depends strongly on the collision (elementary) processes operating, for given external control parameters, between the constituents of the discharge: electrons, ions, molecules, and atoms. Mathematically, these processes are encoded in the collision integrals of the Boltzmann-Poisson equations (see Chapter XY), which are classical equations describing the discharge on the macroscopic length scales defined by the mean-free paths of the various species and the screening length. The dynamics of the elementary processes, however, takes place on the much shorter microscopic scale. It is thus controlled by quantum mechanical principles which will be discussed in this section.

From the quantum-mechanical point of view, see Fig. 9.1 for an illustration, collisions proceed through temporary compound states (1) which form and fragment on the atomic length and time scales [1], in contrast to the macroscopic scales on which typical plasma phenomena such as sheath formation or wave propagation occur. That the scales required to complete the momentum, energy, and particle [2] transfer (rearrangement) defining a collision are well separated from the plasma scales has two profound implications: (i) cross sections

[1] If not stated otherwise, in this section it is implicitly assumed that physical quantities are measured in atomic units, that is, lengths, masses, and charges are given in terms of the Bohr radius a_B, the electron mass m_e, and the elementary charge e, respectively. The unit of energy is then $2R_0$, where R_0 is the Rydberg energy.

[2] The term "particle " denotes either a single "fundamental" particle, having no internal degrees of freedom relevant for the collision process, or a collection of fundamental particles in a bound state; in the latter event the term "fragment" will be also used.

Table 9.1: Typical collisions and their compound states for an electro-negative, diatomic gas. The indices i and f denote initial and final internal states of the molecules, atoms, and ions before and after the collision, respectively.

collisions with compound state AB^-	
(1) $e^- + AB_i \rightarrow AB^- \rightarrow e^- + AB_f$	elastic and inelastic scattering
(2) $e^- + AB_i \rightarrow AB^- \rightarrow 2e^- + AB_f^+$	electron impact ionization
(3) $e^- + AB_i \rightarrow AB^- \rightarrow A_f^- + B_f$	dissociative attachment
(4) $e^- + AB_i \rightarrow AB^- \rightarrow e^- + A_f + B_f$	dissociation
(5) $A^- + B_i \rightarrow AB^- \rightarrow e^- + A_f + B_f$	direct detachment
(6) $A^- + B_i \rightarrow AB^- \rightarrow e^- + AB_f$	associative detachment
collisions with different compound states	
(7) $e^- + A_i^- \rightarrow A^{2-} \rightarrow 2e^- + A_f$	impact detachment
(8) $A_i^- + AB_i^+ \rightarrow A_2B \rightarrow A_f + AB_f$	ion-ion annihilation
(9) $A_i^- + AB_i^+ \rightarrow A_2B \rightarrow A_f + A_f + B_f$	ion-ion annihilation
(10) $A_i^- + AB_i \rightarrow A_2B^- \rightarrow e^- + A_f + AB_f$	direct detachment
(11) $A_i^- + AB_i \rightarrow A_2B^- \rightarrow e^- + A_2B_f$	associative detachment
(12) $e^- + AB_i^+ \rightarrow AB \rightarrow A_f + B_f$	dissociative recombination

measured, for instance, in crossed beam or in swarm experiments, can be used without modifications as input data for plasma modeling and (ii) theoretical calculations of cross sections can neglect the plasma environment, which is a tremendous simplification.

Whereas the physics of a collision is unaffected by the plasma, the reverse is of course not true. Elementary processes determine to a large extend the properties of a plasma (see previous chapters). In the first place, a gas discharge can be only maintained electrically, because electron impact ionization and, for an electro-negative gas, dissociative electron attachment produce positively and negatively charged carriers. Equally important are electron impact excitation and dissociation of molecules. They transfer not only external electric energy into internal energy but, most importantly, they also produce the species which are eventually utilized in the technological application of the discharge: electronically excited species when the discharge is used as a light source or laser and reactive fragments (radicals) when the discharge is employed for surface processing or catalysis.

Technologically interesting gas discharges contain complex molecular gases such as CF_4, CF_3I, C_3F_8, CCl_2F_2, or SF_6 with a multitude of excited and fragmented species. Even simple diatomic molecules, for instance, O_2 or N_2 give rise to a large number of species, with an accordingly large number of elementary processes. Leaving aside elementary processes containing three particles in the entrance channel, which are only relevant at rather high densities, the most common collisions for a generic electro-negative, diatomic gas are shown in Table 9.1 where they are also classified according to the collision compounds controlling the microphysics: AB^-, the compound illustrated on the rhs of Fig. 9.1, A^{2-}, A_2B, A_2B^-, and AB. The branching of the compounds and thus the probabilities for the various collisions (cross sections), depend on the initial energy and on the properties of the compound states at the distance where they have to lock-in into the asymptotic scattering states defining the various collisions.

In view of the great technological and economical impact of reactive gas discharges, it is somewhat surprising, that the number of experimental groups measuring cross sections

for gases of plasma-chemical relevance is rapidly diminishing. Thus, any listing of currently available cross section data must be necessarily incomplete. Since, in addition, the gases of interest change with time, cross section data are not included at all in this section. As far as they exist, they can be found, for instance, in the review article by Brunger and Buckman (2), the monograph by Christophorou and Olthoff (3), and in web-based cross section compilations sponsored by national research institutions and university groups whose activities depend on atomic and molecular collision data. The largest ones, maintained, respectively, by the International Atomic Energy Agency, the American National Institute of Standards and Technology, by Oak Ridge National Laboratory, USA, the Japanese National Institute for Fusion Science, the Weizmann Institute of Science in Israel, and the Université Paris-Sud in Orsay, France, are (4):

1. http://www.iaea.org/programmes/amdis
2. http://physics.nist.gov/PhysRefData/contents.html
3. http://www-cfadc.phy.ornl.gov
4. http://dbshino.nifs.ac.jp
5. http://plasma-gate.weizmann.ac.il/
6. http://gaphyor.lpgp.u-psud.fr

Due to lack of empirical cross section data, theoretical calculations become increasingly important. There are two major lines of attack. One, the ab-initio approach, either attempts to construct parameter-free eigenstates for collision compounds and to match these states to the asymptotic scattering states representing specific collision products (5), or to directly obtain parameter-free scattering matrices from a suitable variational principle (6). Both approaches are extremely time consuming and, so far, have been applied only to a few selected collisions involving molecules with at most three atoms. Even when the formal problems preventing the application to complex molecules are solved in the future, it is hard to imagine a non-expert routinely using an ab-initio package to generate cross sections for as yet unstudied collision processes.

The other, perhaps more valuable approach, as far as plasma-chemical applications are concerned, is the semi-empirical approach. Examples of which are the binary-encounter (7–9) and the Deutsch-Märk (10–12) model for electron impact ionization, the resonance model for dissociative attachment (13; 14), electron-detachment (15; 16), dissociative recombination (17; 18), and vibrational excitation (14; 19), and the Landau-Zener model for ion-ion annihilation (20; 21). Common to all these models is that they attempt to encapsulate the complicated collision dynamics in a few parameters which can be either obtained from electronic structure calculations or from experiments. To some extend these models are ad-hoc, but they have the great virtue to provide clear physical pictures for the collision processes, thereby helping the plasma physicist to develop an intuitive understanding of the microphysics of the discharge.

Despite the great diversity of elementary processes in a gas discharge, this section tries to give an uniform presentation of the subject within the framework of multi-channel scattering theory (22–24) focusing, in particular, on inelastic and reactive collisions. On purpose, cross section formulae are not developed to a point where they could be applied to particular collision processes, because this involves mathematically rather technical (approximate) solutions of the given equations which moreover have to be worked out case-by-case. The details can be found in the original literature. Additional information, in particular with regards to formal aspects of calculating cross sections, can be extracted from the review articles by Rudge (25), Bardsley and Mandl (26), Inokuti (27), Lane (28), Delos (29), Chutjian and coworkers (30), Hahn (31), and Florescu-Mitchell and Mitchell (32).

9.2.1 Fundamental concepts

9.2.1.1 Collision cross section

The kinetic description of a gas discharge is based on a set of Boltzmann equations for the distribution functions $f_i(\mathbf{r}, \mathbf{v}, t)$ of the participating species $i = 1, 2, ..., N$ and those parts of Maxwell's equations which are necessary to describe the electro-magnetic driving of the discharge. For a capacitively coupled radio-frequency discharge, for instance, the equations are

$$\left[\partial_t + \mathbf{v} \cdot \nabla_r - \frac{q_i}{m_i} \nabla_r \Phi \cdot \nabla_v\right] f_i(\mathbf{r}, \mathbf{v}, t) = \sum_p I_i^p[\{f_j\}] \ , \tag{9.1}$$

$$\Delta_r \Phi = -\frac{1}{\epsilon_0} \sum_{i=1}^{N} q_i \int d\mathbf{v} f_i \ , \tag{9.2}$$

where $I_i^p[\{f_j\}]$ is the collision integral due to process p appearing in the Boltzmann equation for species i and depending on the subset $\{f_j\}$ of the distribution functions; Φ is the electric potential [3]. The external driving is in this case simply encoded in the boundary conditions for the Poisson equation; q_i and m_i are the charge and mass of species i, respectively, and ϵ_0 is the dielectric constant of the plasma.

The total number N of species required for the kinetic modeling of a generic electronegative, diatomic gas discharge, can be deduced from Table 9.1. Clearly, besides electrons and molecules of the feed-stock gas AB, atoms A and B, and ions AB^+ and A^- have to be taken into account. In general, it is also necessary to include for the molecular and atomic constituents some excited (meta-stable) states. Thus, in total, $N = N_{AB} + N_A + N_B + N_{AB^+} + N_{A^-} + 1$ species have to considered, where N_σ is the number of excited states kept for the atomic or molecular constituent σ.

Each reaction shown in Table 9.1 gives rise to collision integrals in the Boltzmann equations of the respective reaction educts (species in the entrance channel) and reaction products (species in the exit channel). For elastic scattering, the structure of the collision integral is similar to the one originally derived by Boltzmann (33). The majority of collisions, however, is inelastic and reactive, some involve even more than two reaction products. The corresponding collision integrals have then to be constructed from scratch, using elementary statistical considerations.

Take, for instance, electron impact ionization, where a primary electron scatters off a molecule and produces a secondary electron and a positively charged ion. Assuming the target molecule to be at rest, which is a very good approximation because the molecule is much heavier then the electron, the collision integral in the electron Boltzmann equation due to this process reads (34)

$$\begin{aligned} I_e^I[f_e] &= c_{AB} \Big\{ \int d\mathbf{v}_a d\mathbf{v}'' W^I(\mathbf{v}_a; \mathbf{v}, \mathbf{v}'') f_e(\mathbf{v}_a) + \int d\mathbf{v}_a d\mathbf{v}' W^I(\mathbf{v}_a; \mathbf{v}', \mathbf{v}) f_e(\mathbf{v}_a) \\ &- \int d\mathbf{v}' d\mathbf{v}'' W^I(\mathbf{v}; \mathbf{v}', \mathbf{v}'') f_e(\mathbf{v}) \Big\} \ , \end{aligned} \tag{9.3}$$

where momentum conservation is taken into account, the variables $\mathbf{r}$ and t in the distribution functions are suppressed, and c_{AB} is the concentration of the molecules. The function

[3] In this subsection atomic units are not used.

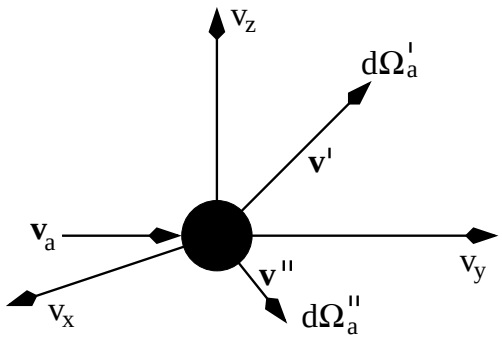

Figure 9.2: Velocity space kinematics of electron impact ionization. Upon impact of the incident electron with velocity vector $\mathbf{v}_a$ two electrons are ejected with velocity vectors $\mathbf{v}'$ and $\mathbf{v}''$, respectively. The solid angles $d\Omega'_a$ and $d\Omega''_a$ corresponding to these two velocities are defined with respect to the direction of $\mathbf{v}_a$. Because of the large mass difference of electrons and molecules, the molecule can be assumed to be at rest.

$W^I(\mathbf{v}_a; \mathbf{v}', \mathbf{v}'')$ is the probability for an incident electron with velocity $\mathbf{v}_a$ to produce two departing electrons with velocities $\mathbf{v}'$ and $\mathbf{v}''$, respectively. Using energy conservation, it can be related to the differential cross section for electron impact ionization

$$\begin{aligned} W^I(\mathbf{v}_a; \mathbf{v}', \mathbf{v}'')d\mathbf{v}'d\mathbf{v}'' &= \frac{1}{2}v_a\sqrt{\frac{v_a^2 - v''^2 - 2E_i/m_e}{v'^2 + v''^2}}q^I(v_a, v'', \Omega'_a, \Omega''_a) \\ &\times \delta(\sqrt{v'^2 + v''^2} - \bar{u})d\Omega'_a d\Omega''_a dv' dv'' \ , \end{aligned} \tag{9.4}$$

with E_i the ionization energy of the molecule, m_e the electron mass, $\bar{u} = \sqrt{v_a^2 - 2E_i/m_e}$, and $q^I(v_a, v'', \Omega'_a, \Omega''_a)$ the differential ionization cross section defined by the relation

$$d\sigma^I = q^I(v_a, v'', \Omega'_a, \Omega''_a)d\Omega'_a d\Omega''_a dv'' \tag{9.5}$$

with $0 \leq v'' \leq \sqrt{v_a^2 - 2E_i/m_e}$ (cf. Fig. 9.2 for notational details).

The sub-nm physics of impact ionization, that is, the momentum, energy and electron transfer during this particular electron-molecule collision, is concealed in the function $q^I(v_a, v'', \Omega'_a, \Omega''_a)$. This statement holds for all processes. The information required about elementary processes reduces thus to a set of (differential) cross sections. The direct measurement of which is tedious, expensive, and, when meta-stable states are involved, which cannot be prepared outside the plasma, sometimes even impossible. It is at this point, where theoretical calculations of cross sections – ab-initio or otherwise – have a great impact.

A systematic solution of the electron Boltzmann equation expands the electron distribution function in terms of velocity space spherical harmonics. The angles Ω'_a and Ω''_a can then be integrated out leading to an hierarchy of Boltzmann equations for the expansion coefficients (34). When the anisotropy of the electron distribution is negligible, the lowest order equation suffices. The collision integral of interest is then

$$q^I(v_a, v'') = \int d\Omega'_a d\Omega''_a q^I(v_a, v'', \Omega'_a, \Omega''_a) \ . \tag{9.6}$$

One more integration would lead to the total ionization cross section,

$$q^I(v_a) = \int dv'' q^I(v_a, v'') \ , \tag{9.7}$$

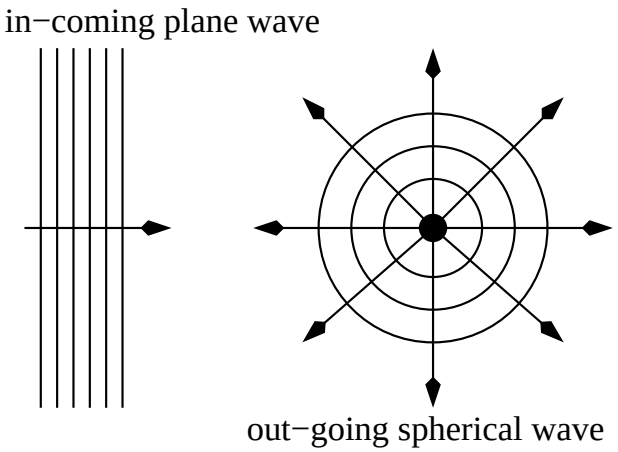

Figure 9.3: Schematic representation of the incoming plane wave and the diverging spherical wave as described by the Lippmann-Schwinger equation (9.9).

which is usually sufficient for a particle-based simulation of the ionization process (see Chapter XY and Ref. (35)).

9.2.1.2 Formal scattering theory

Collisions affecting the charge balance and chemistry of gas discharges change the type, and sometimes even the number, of scattering fragments. An example is electron impact ionization, the process used in the previous section to introduce the concept of a collision cross section. It is an inelastic, break-up collision with an electron and a molecule in the entrance and two electrons and a positive ion in the exit channel. In comparison to the entrance channel, the kinetic energy of the relative motion of the fragments in the exit channel is moreover reduced by the ionization energy of the molecule. Thus, a microscopic description of electron-impact ionization, and likewise of many of the other processes listed in Table 9.1, cannot be based on simple potential scattering theory (elastic scattering). A generalized scattering theory is rather required, capable to account for changes in the internal energy (inelasticity), for rearrangement, and for break-up of the scattering fragments.

The appropriate theoretical framework is quantum-mechanical multichannel scattering theory (22–24). To introduce its essential ingredients, two colliding fragments are considered. In the center-of-mass frame, the total Hamiltonian of the system is

$$H = T_{\rm rel} + H_{\rm int} + V = H_0 + V \ , \tag{9.8}$$

where $T_{\rm rel}$ is the kinetic energy of the relative motion, $H_{\rm int}$ controls the internal degrees of freedom of both fragments, and V is the interaction energy between the two. The Lippmann-Schwinger equation for the scattering state with the boundary conditions shown in Fig. 9.3 reads in Dirac's bra-ket notation

$$|\Psi^{(+)}_{\mathbf{k}\alpha}\rangle = |\Phi_{\mathbf{k}\alpha}\rangle + \frac{1}{E - H_0 + i\eta} V |\Psi^{(+)}_{\mathbf{k}\alpha}\rangle \ , \tag{9.9}$$

where the first term denotes the incoming plane wave in the entrance channel. The channel state, $|\Phi_{\mathbf{k}\alpha}\rangle = |\phi_\alpha\rangle|\mathbf{k}\rangle$, satisfies $(E - H_0)|\Phi_{\mathbf{k}\alpha}\rangle$. Thus, $E = E_{\mathbf{k}\alpha} = k^2/(2\mu) + \omega_\alpha$, where $\mathbf{k}$ is

the relative momentum, ω_α is the internal energy, and μ is the reduced mass of the fragments in the entrance channel.

Quite generally, the scattering amplitude, which in turn determines the differential collision cross section, is defined as the amplitude of the out-going spherical wave emerging from the rhs of Eq. (9.9) for large inter-particle distances. Hence, in order to find the scattering amplitude, Eq. (9.9) has to be expressed in coordinate representation, which is here specified by $\mathbf{r}$, the inter-particle distance, and ρ, the internal coordinates of both particles, and then the limit $r \to \infty$ has to be taken. Normalizing continuum states on the momentum scale leads then to (23; 24)

$$\Psi^{(+)}_{\mathbf{k}\alpha}(\mathbf{r},\rho) \sim \sum_\beta \left[\exp[i\mathbf{k}\cdot\mathbf{r}]\delta_{\alpha\beta} - f(\mathbf{k}'\beta,\mathbf{k}\alpha)\frac{\exp[ik'r]}{r}\right]\phi_\beta(\rho) \tag{9.10}$$

$$= \sum_\beta \left[\exp[i\mathbf{k}\cdot\mathbf{r}]\delta_{\alpha\beta} + \tilde{\psi}^{(+)}_{\mathbf{k}'\beta,\mathbf{k}\alpha}(r)\right]\phi_\beta(\rho) \quad \text{for } r\to\infty\ , \tag{9.11}$$

where $\mathbf{k}'$ is the relative momentum after the collision, and the prefactor in front of the diverging spherical wave,

$$f(\mathbf{k}'\beta,\mathbf{k}\alpha) = -\frac{\mu}{2\pi}\langle\Phi_{\mathbf{k}'\beta}|V|\Psi^{(+)}_{\mathbf{k}\alpha}\rangle\ , \tag{9.12}$$

is the scattering amplitude.

The differential collision cross section is microscopically defined as the ratio of the outgoing particle flux into the solid angle $d\Omega'$ originating from the diverging spherical wave $\tilde{\psi}^{(+)}_{\mathbf{k}'\beta,\mathbf{k}\alpha}(r)$ introduced in Eq. (9.11) and the incoming current density due to the plane wave. Hence,

$$d\sigma = \frac{(\mathbf{j}_{\rm out}\cdot\mathbf{e}_r)r^2 d\Omega'}{k/\mu}\ , \tag{9.13}$$

where $\mathbf{e}_r$ is the unit vector in the direction of $\mathbf{r}$. Inserting $\tilde{\psi}^{(+)}_{\mathbf{k}'\beta,\mathbf{k}\alpha}(r)$ into the quantum-mechanical expression for the particle flux, $\mathbf{j} = (1/(2i\mu))[\psi^*\nabla\psi - \psi\nabla\psi^*]$, yields $\mathbf{j}_{\rm out} = k'|f(\mathbf{k}'\beta,\mathbf{k}\alpha)|^2\mathbf{e}_r/(\mu r^2)$ and thus

$$d\sigma_{\alpha\to\beta} = \frac{k'}{k}|f(\mathbf{k}'\beta,\mathbf{k}\alpha)|^2 d\Omega' = \frac{\mu^2}{(2\pi)^2}\frac{k'}{k}|\langle\Phi_{\mathbf{k}'\beta}|V|\Psi^{(+)}_{\mathbf{k}\alpha}\rangle|^2 d\Omega'\ , \tag{9.14}$$

or, when continuum states are normalized on the energy scale and the identity $V\Psi^{(+)} = t\Phi$ is used (23; 24),

$$d\sigma_{\alpha\to\beta} = \frac{(2\pi)^4}{k^2}|\langle\Phi_{\mathbf{k}'\beta}|t|\Phi_{\mathbf{k}\alpha}\rangle|^2 d\Omega'\ , \tag{9.15}$$

where $t = V + V[E - H_0 + i\eta]^{-1}t$ is the transition operator (T-matrix).

In the derivation of Eq. (9.12) it was implicitly assumed that $\mathbf{r}$ is the inter-particle distance in both the entrance and the exit channel. The particles remain therefore intact in the course of the collision. They may only change their internal state. Hence, the cross section

formulae (9.14) and (9.15) can be only applied to elastic ($\omega_\beta = \omega_\alpha$) and inelastic ($\omega_\beta \neq \omega_\alpha$) scattering.

To obtain the cross section for reactive scattering, the fact has to be included that the type of the particles, and hence the relative and internal coordinates, change during the collision. Thus, writing the Hamiltonian in the form (9.8) is only adequate in the entrance channel. In the exit channel, it is more appropriate to partition the Hamiltonian according to the reaction products and write

$$H = T'_{\rm rel} + H'_{\rm int} + V' = H'_0 + V', \tag{9.16}$$

where $T'_{\rm rel}$, $H'_{\rm int}$, and V' are the relative kinetic energy, the internal energy, and the interaction energy in the exit channel. Then, in addition to Eq. (9.9), the scattering state $|\Psi^{(+)}_{\mathbf{k}\alpha}\rangle$ obeys also an homogeneous Lippmann-Schwinger equation [4],

$$|\Psi^{(+)}_{\mathbf{k}\alpha}\rangle = \frac{1}{E - H'_0 + i\eta} V' |\Psi^{(+)}_{\mathbf{k}\alpha}\rangle \ , \tag{9.17}$$

from which the scattering amplitude in the exit channel (reaction amplitude) can be deduced by the same procedure as before, except that now the coordinate representation with respect to $\mathbf{r}'$ and ρ', the relative and internal coordinates in the exit channel, has to be chosen. In this representation, the scattering state becomes a diverging spherical wave for $r' \to \infty$. The prefactor of which (continuum states normalized on the momentum scale),

$$f'(\mathbf{k}'\beta, \mathbf{k}\alpha) = -\frac{\mu'}{2\pi} \langle \Phi'_{\mathbf{k}'\beta} | V' | \Psi^{(+)}_{\mathbf{k}\alpha} \rangle \ , \tag{9.18}$$

with μ' the reduced mass in the exit channel and $|\Phi'_{\mathbf{k}'\beta}\rangle$ an eigenstate of H'_0, can be identified with the reaction amplitude. Hence, the differential cross section for reactive scattering is given by

$$d\sigma_{\alpha\to\beta} = \frac{\mu}{\mu'} \frac{k'}{k} |f'(\mathbf{k}'\beta, \mathbf{k}\alpha)|^2 d\Omega' = \frac{\mu\mu'}{(2\pi)^2} \frac{k'}{k} |\langle \Phi'_{\mathbf{k}'\beta} | V' | \Psi^{(+)}_{\mathbf{k}\alpha} \rangle|^2 d\Omega' \ , \tag{9.19}$$

where energy conservation enforces now $E = k'^2/(2\mu') + \omega'_\beta = k^2/(2\mu) + \omega_\alpha$. Obviously, Eq. (9.19) reduces to Eq. (9.14) for $V' = V$ which implies $H'_0 = H_0$ and thus $\mathbf{r}' = \mathbf{r}$, $\mu' = \mu$, and $\Phi' = \Phi$.

If the interaction V in the entrance channel is simpler than the interaction V' in the exit channel, it may be more convenient to use the adjoint scattering state, $\langle \Psi^{(-)}_{\mathbf{k}'\beta}|$, which describes an incoming wave in the exit channel. The reaction cross section can then be written as

$$d\sigma_{\alpha\to\beta} = \frac{\mu\mu'}{(2\pi)^2} \frac{k'}{k} |\langle \Psi^{(-)}_{\mathbf{k}'\beta} | V | \Phi_{\mathbf{k}\alpha} \rangle|^2 d\Omega' \ , \tag{9.20}$$

which contains V instead of V'.

The formalism described so far is only applicable to binary collisions, that is, collisions containing two particles in the entrance and exit channel, respectively. The theoretical description of collisions involving three (or more) reaction products (break-up collisions) can

[4] The equation is homogeneous because the incoming wave belongs to a different Hilbert space

be also based on a set of Lippmann-Schwinger equations, but the increased dimensionality of the relative motion requires a substantial extension of the formalism (see Ref. (22)), beyond the scope of this introductory presentation. Additional complications arise for identical particles in a given channel, or when the interaction is long-ranged, as it is, for instance, the case for electron-impact ionization. Ionization cross sections are therefore hardly obtained from rigorous calculations. They are usually estimated from less ambitious, semi-empirical models to be described below.

9.2.1.3 Adiabatic approximation

The formalism described in the previous subsection will be now applied to electron-molecule scattering. To be specific, a diatomic molecule with N electrons is considered. The scattering wavefunctions, $\Psi^{(\pm)}(\mathbf{r}', \mathbf{r}, \mathbf{R})$, from which the scattering amplitudes are obtained, depend then on the N coordinates of the target electrons, which are collectively denoted by $\mathbf{r}'$, the coordinate of the projectile electron $\mathbf{r}$, and the inter-nuclear distance $\mathbf{R}$. In the interest of clarity, spin degrees of freedom are suppressed.

The Lippmann-Schwinger equation for electron-molecule scattering cannot be solved exactly. Approximation schemes, usually based on an expansion of the scattering state in an appropriate basis, are therefore necessary. When the target states, that is, the eigenfunctions of $H^{(N)} = T_R + H_{el}^{(N)}$, where T_R is the kinetic energy of the nuclei and $H_{el}^{(N)}$ is the Hamiltonian for the N target electrons at fixed $\mathbf{R}$, are used, the expansion leads to the close-coupling approximation. Identifying ρ with $(\mathbf{r}', \mathbf{R})$, the close-coupling approximation is basically identical to the channel state representation described in the previous subsection. However, this brute-force approach is not well suited. The number of channels (electronic, vibrational, and rotational), which are all coupled by the Lippmann-Schwinger equation, is too large. In addition, due to the differences in the electronic and nuclear energy scales, the rate of convergence is rather pure.

An approximation scheme accounting for the difference in the energy scales, and thus more appropriate for electron-molecule scattering, is the adiabatic approximation. It expands the scattering state in terms of eigenfunctions of $H_{el}^{(N+1)}$, that is, eigenfunctions of the fixed-nuclei Hamiltonian for the $N+1$ electrons (N target electrons and one projectile electron) of the compound state AB^-, which depend only parametrically on the inter-nuclear distance. Since the dynamic coupling due to the perturbation T_R is usually negligible, only one term contributes to the expansion. The computational costs are thus substantially reduced. In addition, provided the conditions for the validity of the adiabatic approximation are fulfilled, the target can be also described adiabatically. Thus, the target states are Born-Oppenheimer states, which are of course also much easier to determine than the target states needed in a close-coupling calculation.

The adiabatic approximation is valid far away from excitation thresholds and when the collision time is much shorter than the period of nuclear vibration and rotation. It is thus mostly applied to non-resonant electron-molecule scattering. As shown by Shugard and Hazi (36), the differential cross section for electron impact excitation of a diatomic molecule reads for continuum states normalized on the energy scale,

$$d\sigma_{n_i\nu_i J_i \to n_f\nu_f J_f} = \frac{(2\pi)^4}{k_i} |T_{n_f\nu_f J_f, n_i\nu_i J_i}(\Omega_f, \Omega_i)|^2 d\Omega_f \ , \tag{9.21}$$

with Ω_i and Ω_f the solid angles of $\mathbf{k}_i$ and $\mathbf{k}_f$, the electron momenta before and after the

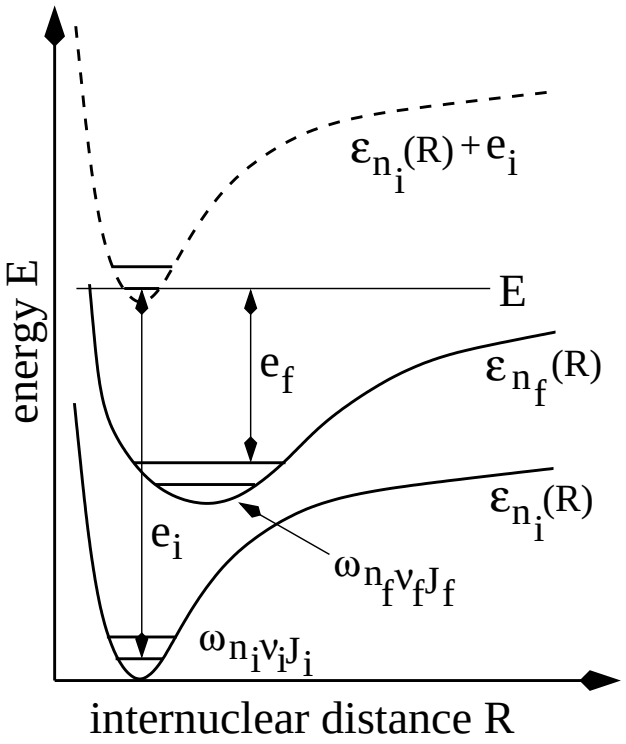

Figure 9.4: Potential energy surface of the initial and final state of electron-impact excitation of a diatomic molecule and the relationship of the various energies occurring in the adiabatic approximation for the scattering cross section. The kinetic energy of the electron before and after the collision is denoted by $e_i = k_i^2/2$ and $e_f = k_f^2/2$, respectively.

collision, respectively. The total scattering amplitude,

$$T_{n_f\nu_f J_f,n_i\nu_i J_i}(\Omega_f,\Omega_i) = \int d\mathbf{R} F^*_{n_f\nu_f J_f}(\mathbf{R}) t_{n_f n_i}(\Omega_f,\Omega_i,\mathbf{R}) F_{n_i\nu_i J_i}(\mathbf{R}) \ , \tag{9.22}$$

is an average of the fixed-nuclei scattering amplitude,

$$t_{n_f n_i}(\Omega_f,\Omega_i,\mathbf{R}) = \frac{k_f^{1/2}}{(2\pi)^{3/2}} \int d\mathbf{r} d\mathbf{r}' \exp[i\mathbf{k}_f\cdot\mathbf{r}] \Phi^*_{n_f}(\mathbf{r}';\mathbf{R}) V(\mathbf{r},\mathbf{r}';\mathbf{R}) \Psi^{(+)}_{\mathcal{E},\Omega,n_i}(\mathbf{r},\mathbf{r}';\mathbf{R}) \ , \tag{9.23}$$

over the ro-vibrational states $F_{n\nu J}(\mathbf{R})$ satisfying

$$\left[T_R + \epsilon_n(R) - \omega_{n\nu J}\right] F_{n\nu J}(\mathbf{R}) = 0 \ , \tag{9.24}$$

where $\omega_{n\nu J}$ is the ro-vibrational energy and $\epsilon_n(R)$ is the potential-energy-surface defined as the eigenvalue of the fixed-nuclei Schrödinger equation for the target electrons

$$\left[H^{(N)}_{el} - \epsilon_n(R)\right] \Phi_n(\mathbf{r}',\mathbf{R}) = 0 \ . \tag{9.25}$$

In view of the discussion of the previous subsection, the structure of the formulae (9.21)-(9.23) should be clear. The physical meaning of the various energies can be deduced from Fig. 9.4. Note, in particular, that the energy $\mathcal{E} = \epsilon_{n_i} + k_i^2/2 = \epsilon_{n_i} + E - \omega_{n_i\nu_i J_i}$ appearing in Eq. (9.23) is only the total electronic energy, for the projectile electron and the N target electrons, in contrast to the total energy E which includes electronic and nuclear degrees of freedom. Ro-vibrational states are characterized by the quantum number n of the electronic state in which the nuclear motion takes place, the vibrational quantum number ν, and the rotational quantum number J. Energy conservation implies $E = k_i^2/2 + \omega_{n_i\nu_i J_i} = k_f^2/2 + \omega_{n_f\nu_f J_f}$.

Within the adiabatic approximation, it is necessary to determine the fixed-nuclei scattering amplitude and the ro-vibrational states of the molecule, which in turn depend on the potential energy surface of the target molecule. The former can be obtained, as a function of $\mathbf{R}$, from the asymptotics of the $N+1$ electron, fixed-nuclei Lippmann-Schwinger equation, which determines $\Psi^{(+)}_{\mathcal{E},\Omega,n_i}(\mathbf{r},\mathbf{r}';\mathbf{R})$, while the latter requires, again as a function of $\mathbf{R}$, the solution of the N electron problem (9.25). In both cases, anti-symmetrized wavefunctions have to be used because of the indistinguishability of electrons. Thus, even when the nuclear motion is split off, the calculation of cross sections for electron-molecule scattering remains a formidable many-body problem (28).

9.2.1.4 Resonant scattering

At electron energies of a few electron volts or less the collision time is long compared to the period of the inter-nuclear motion and the adiabatic approximation fails. The projectile electron is then so slow that it is captured by the molecule giving rise to a bound state of the negatively charged molecular ion, which is the collision compound for electron-molecule scattering [5]. This state interacts with the electron-molecule scattering continuum,

[5] The electronic and vibrational properties of negative ions play therefore an important role in low-temperature gas discharges with $k_B T_e \sim \mathcal{O}(1-10eV)$, even when the gas is not electro-negative, that is, when the negative ion is unstable on the plasma time scale and therefore irrelevant at the kinetic level.

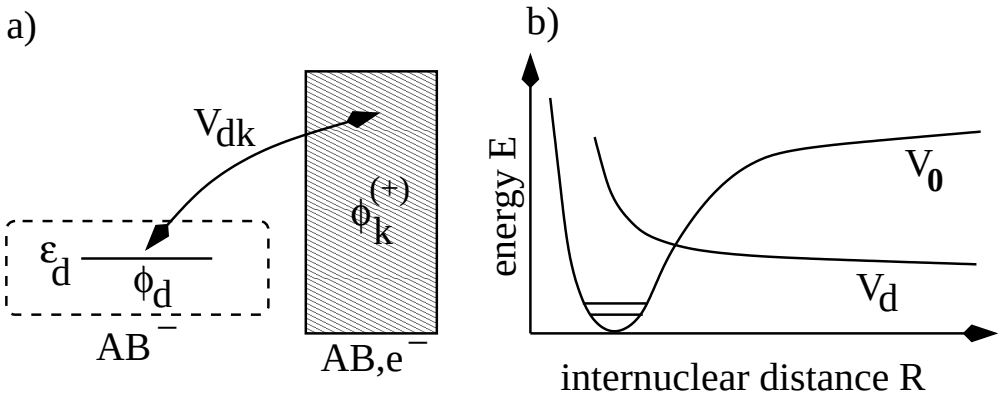

Figure 9.5: Illustration of the effective Hamiltonian (9.26) defining the resonance model.

acquires therefore a finite lifetime, and turns into a quasi-bound (auto-detaching) state. Auto-detaching states play a central role in (vibrational) excitation, attachment, recombination, and detachment collisions. From a theoretical point of view, all these processes can be hence analyzed within a model describing a discrete state (resonance) embedded in a continuum of scattering state.

A particularly elegant derivation of the resonance model for an electron colliding with a diatomic molecule containing N electrons has been given by Domcke (37) who uses many-particle Green functions to reduce the $N+1$ electron scattering problem to an effective single-electron problem. The reduction is achieved by two projections: First, electronic states which are not accessible at the energy considered, are eliminated by introducing an optical potential for the incoming electron. Then, in a second step, the fixed-nuclei T-matrix is split into a rapidly varying part due to the quasi-bound resonant state and a slowly varying background term. The splitting of the T-matrix can be shown to be equivalent to an effective single-electron Hamiltonian at fixed-nuclei describing a resonance coupled to a continuum of states. At the end, the kinetic energy of the nuclei is included and the electronic degrees of freedom are integrated out to obtain an effective Lippmann-Schwinger equation for the nuclear dynamics which, with appropriate boundary conditions, can then be used to calculate the collision cross sections of interest.

It is essential for the formalism that the optical potential supports a resonance and that the resonance can be extracted from the single-electron continuum such that the scattering background contains no spurious resonances. The many electron problem is then completely buried in an optical potential, which can be calculated separately using, for instance, many-body perturbation theory (38). In principle, the formalism can handle more than one resonance as well as electronically inelastic processes (39). So far, however, it has been only applied to electronically elastic collisions involving a single resonance and a single potential energy surface for the nuclear motion of the target.

The effective Hamiltonian, visualized in Fig. 9.5, reads

$$\begin{aligned} H &= H_0 + V \\ H_0 &= |\phi_d\rangle \left[T_R + V_d \right] \langle \phi_d| + \int k dk d\Omega_k |\phi_{\mathbf{k}}^{(+)}\rangle \left[T_R + V_0 + \frac{k^2}{2} \right] \langle \phi_{\mathbf{k}}^{(+)}| \\ V &= \int k dk d\Omega_k \left[|\phi_d\rangle V_{d\mathbf{k}} \langle \phi_{\mathbf{k}}^{(+)}| + \text{h.c.} \right] , \end{aligned} \tag{9.26}$$

where $|\phi_d\rangle$ is the resonant state and $|\phi_{\mathbf{k}}^{(+)}\rangle$ are the scattering states orthogonal to $|\phi_d\rangle$. The coupling between the two types of states is given by $V_{d\mathbf{k}} = \langle\phi_d|H_{el}|\phi_{\mathbf{k}}^{(+)}\rangle$, where $H_{el} = -\nabla^2/2 + V_{\rm opt}$ is the Hamiltonian for a single electron in the optical potential $V_{\rm opt}$; $V_d = \langle\phi_d|H_{el}|\phi_d\rangle + V_0$ is an operator specifying the potential of the resonant state and V_0 is the corresponding operator for the potential of the target molecule.

The Hamiltonian (9.26), and thus the Lippmann-Schwinger equation associated with it, operate in the combined Hilbert space of the scattered electron and the two nuclei. Projecting out the electron, switching to the coordinate representation with respect to the inter-nuclear distance, and using out-going wave boundary conditions yields, when rotations of the molecule are ignored, a Lippmann-Schwinger equation,

$$\left[E + \frac{1}{2\mu}\frac{d^2}{dR^2} - V_d(R)\right]\Psi_{dE}^{(+)}(R) - \int dR' F^{(+)}(R,R',E)\Psi_{dE}^{(+)}(R') = J(R)\ , \tag{9.27}$$

with a kernel

$$F^{(+)}(R,R',E) = \int k dk d\Omega_k V_{d\mathbf{k}}(R) G^{(+)}(R,R',E-k^2/2) V_{d\mathbf{k}}^*(R')\ , \tag{9.28}$$

where

$$G^{(+)}(R,R',E) = \langle R|\big[E + \frac{1}{2\mu}\frac{d^2}{dR^2} - V_0(R) + i\eta\big]^{-1}|R'\rangle \tag{9.29}$$

is the Green function for the nuclear motion on the potential energy surface of the target, $V_0(R) = \langle R|V_0|R\rangle$, and μ is the reduced mass of the nuclei; $V_d(R) = \langle R|V_d|R\rangle = \epsilon_d(R) + V_0(R)$ is the potential energy surface of the resonant state and $V_{d\mathbf{k}}(R) = \langle R|V_{d\mathbf{k}}|R\rangle$. The inhomogeneity $J(R)$ on the rhs of Eq. (9.27) depends on the boundary conditions. It will be discussed below for particular collision processes.

Equation (9.27) is an effective Lippmann-Schwinger equation for the nuclear dynamics in the energy-dependent, nonlocal, and complex potential of the resonant state. To make this more explicit, $G_0^{(+)}(R,R',E)$ is expressed in terms of a complete set of target nuclear wavefunctions $\chi_\nu(R)$. Employing Dirac's identity and assuming that the interaction between the resonance and the scattering continuum depends only on k (isotropic interaction), leads to

$$F^{(+)}(R,R';E) = \Delta(R,R';E) - \frac{i}{2}\Gamma(R,R';E) \tag{9.30}$$

with

$$\Delta(R,R';E) = 4\pi\sum_\nu\ {\rm P}\!\int dE' \frac{V_{dE'}(R)\chi_\nu^*(R)\chi_\nu(R')V_{dE'}^*(R')}{E-\omega_\nu-E'} \tag{9.31}$$

and

$$\Gamma(R,R';E) = 8\pi\sum_\nu V_{dE-\omega_\nu}(R)\chi_\nu^*(R)\chi_\nu(R')V_{dE-\omega_\nu}^*(R')\ , \tag{9.32}$$

where the symbol "P" denotes the principal value of the integral and ω_ν stands for the vibrational energies of the target molecule.

The inverse of $\Gamma(R, R'; E)$ is the lifetime of the resonance. As expected, the auto-detaching property of the resonance arises from its coupling to the scattering continuum. In principle, the resonance has a finite lifetime even in the absence of this coupling because the optical potential, $V_{\rm opt}$, is complex. Its imaginary part induces therefore a lifetime. This contribution, however, is much smaller than the one due to V_{dE}. Hence, it is usually neglected.

The non-locality of the potential complicates the numerical solution of Eq. (9.27). In the early applications of the resonance model (13–18; 26), the nonlocal potential was thus replaced by a local one. The local approximation can be obtained from Eqs. (9.31)–(9.32) by identifying the energy available for the scattered electron with an effective resonance energy: $E - \omega_\nu \approx E_{\rm res}(R)$ (37). The completeness of the vibrational target states can then be used to obtain $\Delta(R, R'; E) = \Delta_L(R)\delta(R - R')$ and $\Gamma(R, R'; E) = \Gamma_L(R)\delta(R - R')$ with

$$\Gamma_L(R) = 8\pi |V_{dE_{\rm res}(R)}(R)|^2, \qquad \Delta_L(R) = 4\pi \ {\rm P}\!\int \frac{|V_{dE_{\rm res}(R)}(R)|^2}{E_{\rm res}(R) - E'} \ , \tag{9.33}$$

which reduces the Lippmann-Schwinger equation to an ordinary differential equation:

$$\left[E + \frac{1}{2\mu}\frac{d^2}{dR^2} - V_0(R) - \Delta_L(R) + \frac{i}{2}\Gamma_L(R)\right]\Psi^{(+)}_{dE}(R) = J(R) \ . \tag{9.34}$$

The scattering cross sections derived from Eq. (9.27) or Eq. (9.34) are only as good as the optical potential, $V_{\rm opt}$, the potential energy surfaces $V_0(R)$ and $V_d(R)$, and the coupling function $V_{d\mathbf{k}}(R)$. These quantities have to be obtained from separate calculations, ideally using ab-initio techniques of molecular structure theory, or directly from experiments. But even then, the cross sections form the resonance model are semi-empirical in the sense that a priori assumptions about the relevance or irrelevance of molecular ion and target states have to be made from the very beginning. This weakness of the model, however, leads at the same time to its strength: Technically tractable equations, with an intuitive physical interpretation, which, in the local approximation, can be even solved analytically with semi-classical techniques (40–42).

9.2.2 Typical processes

Now representative elementary processes are discussed in more detail, focusing, in particular, on reactive and inelastic collisions, which change the internal energy and composition of the scattering fragments. Elastic scattering between the various species is not explicitly included although the associated cross sections are usually much larger than the cross sections for inelastic and reactive collisions combined. But they only randomize the directed motion of the electrons in the electric field. The thereby induced changes of the electron energy distribution function affects the plasma-chemistry only indirectly, in as much as an increase of energy in the electronic subsystem makes certain collisions more probable than others.

9.2.2.1 Production of ions

The main production processes for ions in a molecular, electro-negative gas discharge are electron impact ionization and dissociative electron attachment. Both processes share the same compound state, AB^-, but the former leads to positive molecular ions whereas the latter to negative atomic ions. Impact ionization is in addition also the main source for

electrons which, depending on their energy, trigger a multitude of excitation and dissociation collisions.

Electron impact ionization is similar to electronic excitation (see below), except that the excited state belongs to the two-electron continuum. In the notation of the previous subsection, the differential cross section is thus proportional to the modulus of the reaction amplitude squared,

$$d\sigma^{\mathrm{I}}_{\alpha\to\beta} \sim |\langle\Phi'_{\beta\mathbf{k}_1\mathbf{k}_2}|V'|\Psi^{(+)}_{\alpha\mathbf{k}}\rangle|^2 d\Omega_1 d\Omega_2 dE_2 \ , \tag{9.35}$$

where Ω_1 is the solid angle associated with $\mathbf{k}_1$, the momentum of the primary electron, Ω_2 is the solid angle associated with $\mathbf{k}_2$, the momentum of the secondary electron, and E_2 is the energy of the secondary electron. The exit channel state, $|\Phi'_{\beta\mathbf{k}_1\mathbf{k}_2}\rangle = |\phi'^{\mathrm{AB}^+}_{\beta}\psi'_{\mathbf{k}_1\mathbf{k}_2}\rangle$, describes the internal state of the positive ion and the six-dimensional relative motion between the two electrons and the ion, which is controlled by V', that is, the Coulomb interaction of the primary and secondary electron with each other and with the positive ion. The entrance channel of the set of Lippmann-Schwinger equations satisfied by the scattering state $|\Psi^{(+)}_{\alpha\mathbf{k}}\rangle$ contains an inhomogeneity, $|\Phi_{\alpha\mathbf{k}}\rangle = |\phi^{\mathrm{AB}}_{\alpha}\rangle|\mathbf{k}\rangle$, where $|\phi^{\mathrm{AB}}_{\alpha}\rangle$ is the initial state of the molecule and $|\mathbf{k}\rangle$ is the plane wave representing the relative motion of the initial electron and the molecule.

From a rigorous mathematical point of view, the exact two-electron scattering state in the field of a positive ion is unknown. Hence, exact calculations of electron impact ionization cross sections are not available, even for atoms, where complications due to the nuclear dynamics are absent. Perturbative treatments, based, for instance, on the distorted Born approximation, which replaces $\psi'_{\mathbf{k}_1\mathbf{k}_2}$ by a plane wave for the primary electron and a Coulomb wave for the secondary electron, are possible, provided the velocity of the incident electron is much larger than the velocities of the electrons bound in the molecule. Exchange and correlation effects can then be ignored and the calculation of cross sections for electron-impact ionization reduces essentially to the calculation of photo-ionization cross sections. This approach, due originally to Bethe (7) and reviewed by Rudge (25) and Inokuti (27), fails at low electron energies. But in that region, Vriens' binary-encounter model (8) can be used. It assumes that the primary electron interacts pairwise with target electrons, leaving the remaining electrons and the nuclear dynamics undisturbed. The ionization cross section is then basically the Mott cross section for the collision of two electrons, appropriately modified by the binding and kinetic energies of the target electrons.

The semi-empirical *Kim-Rudd model* for electron impact ionization (9) combines the Bethe model with the binary-encounter model. For an individual orbital, the ionization cross section is then given by

$$\sigma^I(e) = \frac{S}{e+u+1}\left\{\frac{1}{2}Q\left(1-\frac{1}{e^2}\right)\ln e + (2-Q)\left[1-\frac{1}{e}-\frac{\ln e}{e+1}\right]\right\} , \tag{9.36}$$

with $e = E/B$ and $u = U/B$, where E is the kinetic energy of the incident electron, U is the average kinetic energy of the orbital, and B is the binding energy of the orbital. The remaining quantities are $S = 4\pi N/B^2$ and $Q = 2BM_i^2/N$ with N the orbital occupation number and M_i an integral over the differential oscillator strength defined in Ref. (9). The results obtained from Eq. (9.36) are surprisingly good.

Another widely used semi-empirical model for electron impact ionization is the *Deutsch-Märk model* (10–12). It uses cross sections for the atomic constituents of the molecules and sums them up according to the atomic population of the molecular orbitals which is obtained

from a Mullikan population analysis. The total ionization cross section can then be written as

$$\sigma^I(E) = \sum_{n,l,i} g_{i,nl} \pi r_{i,nl}^2 N_{i,nl} f(e_{i,nl}) \tag{9.37}$$

with $r_{i,nl}^2$ the mean square radius of the n,l-th sub-shell of the constituent i, $N_{i,nl}$ the occupancy of that sub-shell, $g_{i,nl}$ weighting factors which have to be determined empirically using reliable atomic cross section data, and a function

$$f(e_{i,nl}) = \frac{1}{e_{i,nl}} \left(\frac{e_{i,nl}-1}{e_{i,nl}+1} \right)^{3/2} \left\{ 1 + \frac{2}{3} \left(1 - \frac{1}{2e_{i,nl}} \right) \ln \left[2.7 + \sqrt{e_{i,nl}-1} \right] \right\} , \tag{9.38}$$

which describes the energy dependence of the cross section. The quantity $e_{i,nl} = E/B_{i,nl}$ with $B_{i,nl}$ the ionization energy of the considered sub-shell of the i-th constituent. More elaborate versions of the Deutsch-Märk model account also for the different angular symmetries of the sub-shells (10).

The cross sections for impact ionization are fairly large because it is an optically allowed process (this can be most clearly seen when the Born approximation is applied) and the energy in the final state can be distributed among the two electrons in infinite many ways. Hence, a gas discharge usually contains a high concentration of electrons and positive ions.

Negative ions are produced by *dissociative attachment*, which is a resonant process due to the collision of a slow electron with a (in general) vibrationally excited molecule, where the compound state AB^- dissociates into a negative ion A^- and a neutral atom B. In principle, it would be also conceivable that the incident electron is permanently bound to the molecule and a negative molecular ion is formed. A necessary condition for this to happen would be that the relevant potential energy surface of the AB^- state is bonding and has a minimum outside the "potential well " corresponding to the electronic groundstate of the AB molecule. However, the electron is always captured above the re-detachment threshold, that is, the molecular ion is initially in an excited state. It can be only stabilized when it looses or disperses excess energy. The former occurs through collisions with other molecules or the wall while the latter takes place through vibrational modes of the AB^- compound. In most cases, these processes are not very efficient and the AB^- state is only a short-lived resonance not affecting the macrophysics of the discharge.

As pointed out by O'Malley (13) and others (14), dissociative attachment most likely occurs when an anti-bonding state of the collision compound AB^- crosses the initial potential energy surface of the AB molecule as schematically shown in Fig. 9.6. This is the typical situation for the resonance model to be applicable. Thus, with the appropriate identifications and boundary conditions, the cross section for dissociative attachment can be calculated from the effective Hamiltonian (9.26).

The natural boundary conditions for dissociative attachment are an incoming plane wave for the relative electron-molecule motion and an outgoing spherical wave in the relative (A^-, B) motion. The formula for the attachment cross section, which is an reaction cross section [cp. with Eq. (9.19)], would then however contain the interaction in the exit channel, that is, the interaction between A^- and B, which is not part of the resonance model. This complication can be avoided when the adjoint scattering problem is considered, whose boundary conditions are an incoming plane wave in the (A^-, B) channel and an outgoing spherical wave in the electron-molecule channel. The cross section contains then the interaction between the resonant state and the $e - AB$ scattering continuum. Specifying Eq. (9.20)

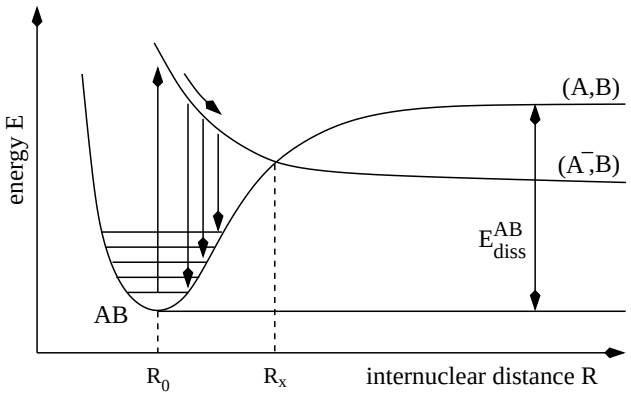

Figure 9.6: Schematic representation of the relevant potential energy surfaces for dissociative attachment. For simplicity, it is assumed that the molecule AB is initially in the vibrational groundstate, although this is usually not the case. The electron is thus captured at $R = R_0$, where R_0 is the equilibrium distance of the two nuclei (upward directed vertical arrow). The thereby created AB^- compound is envisaged to be in an anti-bonding state whose potential energy surface crosses at $R = R_x$ the potential energy surface of the AB state. For $R < R_x$ the compound state has thus a finite probability to decay (downward directed vertical arrows). However, provided the state survives until the nuclear distance $R > R_x$, it asymptotically reaches the (A^-, B) dissociation limit and dissociative attachment is completed.

to the present case, the differential cross section for dissociative attachment becomes

$$d\sigma_{\nu_i}^{\mathrm{DA}} = \frac{mM}{(2\pi)^2}\frac{K}{k_i}\left|\int dR\left[\Psi_{dE}^{(-)}(R)\right]^* V_{dk}^*(R)\chi_{\nu_i}(R)\right|^2 d\Omega_K \ , \tag{9.39}$$

where m and k are the reduced mass and the relative momentum of the (e^-, AB) system, respectively, M and K are the corresponding quantities in the (A^-, B) system, $\chi_{\nu_i}(R)$ is the vibrational state of the molecule, and $\Psi_{dE}^{(-)}(R)$ is the scattering state satisfying the complex conjugate of Eq. (9.27) with $V_d(R) = V_{\mathrm{AB}^-}(R)$, $V_0(R) = V_{\mathrm{AB}}(R)$, $V_{dk}(R)$ the interaction between the anti-bonding AB^- state and the electron-molecule scattering continuum, and $J(R) = [V_d(\infty) - V_d(R)]\exp[iKR]$. The total energy available for the collision $E = k^2/2 + \omega_{\nu_i} = K^2/(2M) + \omega_{A^-} + \omega_B$, where ω_{A^-} and ω_B denote the internal energies of the ion and atom, respectively, and ω_{ν_i} is the vibrational energy of the molecule.

In order to avoid additional indices, quantum numbers for the internal state of the (A^-, B) system are suppressed and rotations of the molecule are also ignored. Because the period of rotation is much longer than the collision time, rotations could be included within the adiabatic approximation. Finally, provided the kinetic energy of the incident electron, $k^2/2$, is much larger than the vibrational energy of the target, ω_{ν_i}, the local approximation could be employed, that is, Eq. (9.34) could be used instead Eq. (9.27). Further details about the calculation of electron attachment cross sections can be found in the review article by Chutjian and collaborators (30).

Bardsley and coworkers (14) have shown that within the semi-classical approximation $d\sigma_{\nu_i}/d\Omega_K$ factorizes into a capture cross section, which describes the formation of the compound state, and a survival probability for that state. The semi-classical calculation moreover shows that the capture cross section increases faster with temperature than the survival

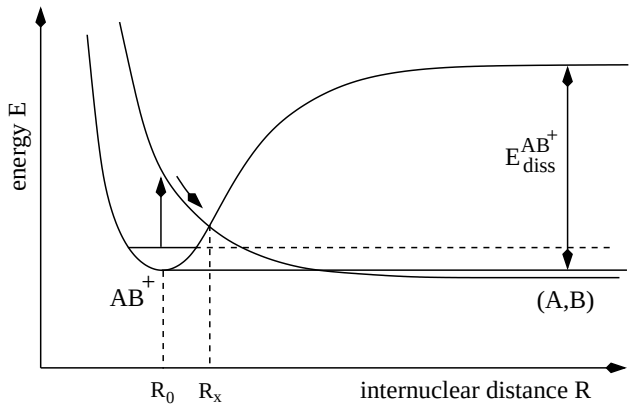

Figure 9.7: Dissociative recombination occurs when an anti-bonding potential energy surface of the (excited) molecule, $V_{AB}(R)$, crosses the potential energy surface of the positive molecular ion AB^+. Although the states involved are different, the mechanism is similar to dissociative attachment. When the molecule, which is the collision compound in this case, survives auto-detachment for $R < R_x$, it may reach the (A, B) dissociation limit. As a result, dissociative recombination takes place.

probability decreases. Thus, the attachment cross section increases with temperature. It is however always one or two orders of magnitude smaller than the cross section for the corresponding elastic electron-molecule scattering.

9.2.2.2 Destruction of ions

Whereas in an electro-negative gas discharge only two processes are primarily responsible for the production of ions and electrons – electron impact ionization and dissociative attachment – a large number of processes may lead to the destruction of ions and electrons (see Table 9.1). Depending on the parameters of the discharge, the loss of ions may be due primarily to recombination or detachment. Recombination may furthermore occur between positive ions and electrons or between positive and negative ions (annihilation). For molecular positive ions, the former process is usually accompanied by dissociation and is thus called dissociative recombination. Ion-ion annihilation, on the other hand, is in most cases only a charge transfer, which does not lead to a rearrangement of the nuclei. Finally, detachment of negative ions can be either initiated by electrons or by neutrals. Electron-induced detachment is similar to electron impact ionization whereas detachment due to (molecular) neutrals may lead to dissociation, as well as, when the neutral is in a meta-stable state, to association.

Dissociative recombination is triggered by slow electrons. It is thus a resonant process, similar to dissociative attachment. Very often, it is the dominant loss process for positive ions and electrons with relatively large cross sections because at least one of the atomic fragments in the exit channel is usually in an excited state implying that the energy in the exit channel can be distributed in many different ways (32).

The resonance model for dissociative recombination, originally proposed by Bardsley (17; 18), is based on the potential energy surface diagram shown in Fig. 9.7. The most favorable situation for the process to take place is when an anti-bonding potential energy surface of the molecule AB, which is the collision compound for this reaction, crosses the potential energy surface of the positive ion and is for large inter-nuclear distances below the vibrational ground state of the ion. This is, for instance, the case for H_2^+, N_2^+, and O_2^+.

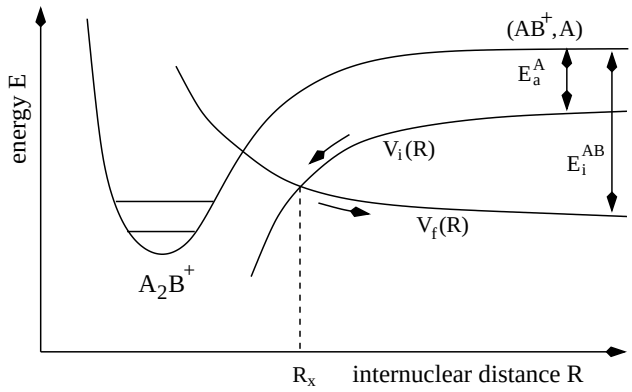

Figure 9.8: Relation of the potential energy surfaces typical for ion-ion annihilation. In the entrance channel, the nuclear dynamics is governed by $V_i(R)$, the potential energy surface of the (AB^+, A^-) configuration, whereas the dynamics in the exit channel is controlled by $V_f(R)$, which is the potential energy surface of the (AB, A) configuration. The strong mixing of the two configurations encoded in $V(R)$ (see Eq. (9.42)) is maximal at $R = R_x$. Both, $V_i(R)$ and $V_f(R)$, belong to the collision compound A_2B. The potential energy surface for the A_2B^+ molecule is also shown. It allows to define the relevant energies: the ionization energy of the AB molecule, E_{ion}^{AB}, and electron affinity of the A atom, E_a^A.

The cross section for dissociative recombination can then be casted into the form (9.39), with M and K the reduced mass and the relative momentum of the (A, B) system, respectively, m and k the corresponding quantities of the (e^-, AB^+) system, $\chi_{\nu_i}(R)$ the initial vibrational state of AB^+, and $\Psi_{dE}^{(-)}(R)$ the solution of the complex conjugate to Eq. (9.27) with $V_d(R) = V_{AB}(R)$, $V_0(R) = V_{AB^+}(R)$, and $V_{dk}(R)$ the interaction between the AB state and the $e^- - AB^+$ scattering continuum. The inhomogeneity representing the boundary condition, $J(R) = [V_d(\infty) - V_d(R)]\Phi_K^C(R)$, contains now a Coulomb wave, $\Phi_K^C(R)$, because the scattering continuum is for two charged particles: an electron and a positive ion. More sophisticated approaches use quantum-defects to characterize the scattering states (43; 44).

In electro-negative gas discharges, there is an additional recombination channel: *Ion-ion annihilation*. The potential energy surface diagram relevant for this process is shown in Fig. 9.8. The essential point is that at an inter-nuclear spacing $R = R_x$ the potential energy surface for the (A^-, AB^+) configuration, which decreases with decreasing R because of the Coulomb attraction between the two ions, crosses an anti-bonding potential energy surface of the A_2B collision compound. At this separation, the probability for the system to switch from the (A^-, AB^+) to the (A, AB) configuration is particularly high. Based on this observation, a semi-empirical Landau-Zener model can be constructed which relates the cross section for ion-ion annihilation to the ionization energy of the AB molecule and the electron affinity of the A atom (see Fig. 9.8).

The *Landau-Zener model* illustrates quite nicely how semi-empirical models encode complicated processes in a few physically intuitive parameters. In contrast to the processes discussed so far, where the relevant nuclear dynamics took place on a single potential energy surface, ion-ion annihilation forces the nuclei to switch between two potential energy surfaces of the collision compound. The minimal theoretical model is therefore based on two coupled Lippmann-Schwinger equations for the relative motion of the nuclei. The Landau-Zener model is the semi-classical approximation to this set of equations. Following Olson (20), the

total ion-ion annihilation cross section is then given by

$$\sigma^{\mathrm{IIA}}(E) = 4\pi R_x^2 \left[1 + \frac{\Delta E}{E}\right] F(\lambda) \ , \tag{9.40}$$

with

$$F(\lambda) = \int_1^\infty dx \ x^3 \exp(-\lambda x) \left[1 - \exp(-\lambda x)\right] \tag{9.41}$$

and

$$\lambda = 2\pi \sqrt{\frac{M}{2}} \frac{|V(R_x)|^2}{|V_i' - V_f'|\sqrt{E + \Delta E}} \ , \tag{9.42}$$

where E and M are the kinetic energy and the reduced mass of the relative motion of the (A^-, AB^+) system, ΔE is the energy gain due to annihilation, $V(R_x)$ is the interaction between the (A^-, AB^+) and (A, AB) configurations at $R = R_x$, and $V_{i,f}' = dV_{i,f}(R_x)/dR$ with $V_i(R)$ and $V_f(R)$ the potential energy surfaces of the (A^-, AB^+) and (A, AB) system, respectively.

Equation (9.40) can be developed further, by recalling that $V_i(R) \sim R^{-1}$ (Coulomb interaction between A^- and AB^+) and $V_f(R) \sim r^{-n}$ with $n > 1$ (polarization interaction between A and AB). Hence, for large enough R_x, $|V_i' - V_f'| \approx R_x^{-1}$ and $\Delta E \approx -U_i(R_x) = R_x^{-1}$. Usually, $\Delta E \gg E$. Combining all this leads to $\lambda \approx \sqrt{2M}\pi R_x^{5/2}|V(R_x)|^2$ (20). Since $F(\lambda)$ approaches its maximal value $F_{max} \approx 0.1$ at $\lambda_{max} \approx 0.424$, a rough estimate for the annihilation cross section is

$$\sigma^{\mathrm{IIA}}(E) \approx 1.3 R_x^2 \left[1 + \frac{1}{R_x E}\right] \tag{9.43}$$

with R_x determined from $\lambda_{max} = \sqrt{2M}\pi R_x^{5/2}|V(R_x)|^2$ or from empirical cross section data for high energies where $E \gg R_x^{-1}$ and $\sigma(E) \to 1.3R_x^2$. To determine $V(R_x)$ is not trivial. Ideally, it can be parameterized in terms of an effective ionization energy E_i^{AB} of the AB molecule and the electron affinity E_a^A of the A atom. Olson and coworker (21) obtain for large inter-nuclear distances $V(R) = 1.044\sqrt{E_i^{AB} E_a^A}\sqrt{q}\bar{R}\exp[-0.857\bar{R}]$ with $\bar{R} = 0.5(\sqrt{2E_a^A} + \sqrt{2E_i^{AB}})R$ and q the Franck-Condon factor that represents the overlap of the vibrational states (see below). In order to apply this formula, the ionization potential and the electron affinity have to be known. For atomic negative ions this is no problem. But for molecular negative ions this can be subtle because the ion may be in an (unknown) excited state. Fortunately, molecular negative ions have a rather short lifetime, as discussed before. They are thus not of major concern in the commonly used gas discharges.

For molecular positive ions, *dissociative ion-ion annihilation* may be also possible. It contains two relative motions in the exit channel and is thus much harder to analyze theoretically. Experimentally, it is not always possible to discriminate between this process and the charge-transfer-type reaction discussed in the previous paragraphs. The energy dependence of the two cross sections is however essentially the same, except that they reach the constant value at different energies. Thus, when R_x is determined from the high energy asymptotics of empirical data, the annihilation cross section is in fact an effective cross section, comprising both charge-transfer-type and dissociative ion-ion annihilation.

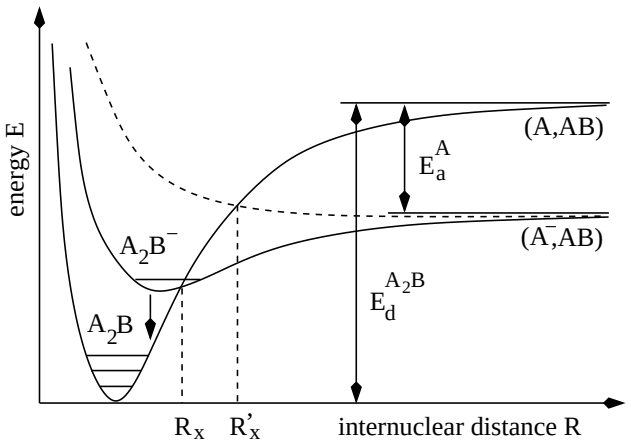

Figure 9.9: Illustration of associative detachment. The potential energy surface of a bonding state of the collision compound A_2B^- crosses the potential energy surface of the A_2B molecule. Auto-detachment of the compound state produces then an electron and a vibrationally excited A_2B molecule. Also shown is an anti-bonding A_2B^- state (dashed line). Detachment may also occur from such a state, but then the initial kinetic energy of the (A^-, AB) system has to be larger than $V_{A_2B^-}(R'_x) - V_{A_2B^-}(\infty)$.

In contrast to positive ions, negative ions can be also destroyed by slow collisions with neutral particles (detachment). To be specific, *associative detachment* of negative ions due to molecules is discussed. Microscopically, it is a resonant process similar to dissociative attachment and dissociative recombination. An auto-detaching, resonant state plays thus an important role. In Fig. 9.9 the relevant potential energy surfaces are shown. The asymptotically stable configuration (A^-, AB) changes with decreasing R into a quasi-bound, resonant collision compound, A_2B^-, from which the electron auto-detaches, leaving behind a free electron and a neutral particle in an excited vibrational state (16–18).

The differential cross section for this process can be obtained from the resonance model, using as boundary conditions an incoming plane wave in the (A^-, AB) channel and an outgoing spherical wave in the (e^-, A_2B) channel. Normalizing continuum states on the energy scale and applying Eq. (9.19) leads to

$$d\sigma_{\nu_f}^{\mathrm{AD}} = \frac{(2\pi)^4}{K^2} \left| \int dR \chi_{\nu_f}^*(R) V_{dk}^*(R) \Psi_{dE}^{(+)}(R) \right|^2 d\Omega_{k_f} \ , \tag{9.44}$$

where $\chi_{\nu_f}(R)$ is the vibrational state of the A_2B molecule and $\Psi_{dE}^{(+)}$ satisfies Eq. (9.27) with $V_d(R) = V_{A_2B^-}(R)$, $V_0(R) = V_{A_2B}(R)$, and $V_{dk}(R)$ the interaction between the quasi-bound A_2B^- state and the $e^- - A_2B$ scattering continuum. The inhomogeneity is $J(R) = [V_d(\infty) - V_d(R)]\Phi_K(R)$ with $\Phi_K(R)$ a plane wave for the relative motion of the (A^-, AB) system. Energy conservation enforces $E = K^2/(2M) + V_d(\infty) = k^2/(2m) + \omega_{\nu_f}$ where M and m are the reduced masses of the (A^-, AB) and the (e^-, A_2B) system, respectively. Notice, since $d\sigma_{\nu_f}^{\mathrm{AD}}$ is a differential cross section for reactive scattering, the interaction in the exit channel, V_{dk}, appears in Eq. (9.44), as it should be.

The most favorable situation for associative detachment is when the potential energy surface of the neutral molecule in the exit channel supports a bound state whose dissociation energy $E_{\mathrm{d}}^{A_2B}$ is larger than the electron affinity E_{a}^{A} of the A atom. This situation is shown in

Fig. 9.9. Provided detachment is mediated by an attractive state of the collision compound, it takes place even for vanishing initial kinetic energy in the (A^-, AB) channel. If this is the case, detachment is a very efficient loss channel for negative ions, even at low temperatures. If, on the other hand, the compound state is anti-bonding, associative detachment occurs only when the initial kinetic energy of the colliding particles is larger than $V_d(R'_x) - V_d(\infty)$, where R'_x is the point where the repulsive potential energy surface crosses $V_0(R)$.

9.2.2.3 Excitation of internal degrees

The chemistry and charge balance of a gas discharge is also affected by inelastic collisions, that is, collisions which increase the internal energy of molecules, atoms, and ions. Excited (meta-stable) particles are reactive and participate in basically all particle number changing collisions. In low temperature gas discharges, vibrationally excited molecules play a particularly important role, because, for typical operating conditions, they are efficiently produced by resonant electron-molecule scattering.

The kinetic energy of electrons in a low-temperature gas discharge is typically a few electron volts. At these energies, the electron-molecule collision time is rather long, favoring therefore resonant enhancement of the collision. The cross section for *vibrational excitation* of molecules is thus given by Eq. (9.14) with the scattering state obtained from the resonance model. Specifically for continuum states normalized on the energy scale, the cross section becomes

$$d\sigma^{\rm VE}_{\nu_i\to\nu_f} = \frac{(2\pi)^4}{k_i^2}\left|\int dR \chi^*_{\nu_f}(R) V^*_{d\mathbf{k}_f}(R)\Psi^{(+)}_{dE}(R)\right|^2 d\Omega_f \ , \tag{9.45}$$

where $\chi_{\nu_f}(R)$ is the vibrational state of the molecule after the collision and $\Psi^{(+)}_{dE}(R)$ is the solution of the effective Lippmann-Schwinger equation (9.27) with $V_d(R) = V_{AB^-}(R)$, $V_0(R) = V_{AB}(R)$, $V_{dk}(R)$ the interaction between the resonant AB^- state and the electron-molecule scattering continuum, and $J(R) = V_{d\mathbf{k}_i}(R)\chi_{\nu_i}(R)$. Energy conservation implies $E = k_i^2/(2\mu) + \omega_{\nu_i} = k_f^2/(2\mu) + \omega_{\nu_f}$ with μ the reduced electron-molecule mass.

The shape of the vibrational excitation cross section depends on the imaginary part of $F(R, R'; E)$, that is, on $\Gamma(R, R'; E)$ (see Eqs. (9.28) and (9.30)). When it is large compared to the inverse of the period of vibration in the resonant state, that is, for a short lived resonance, the cross section is smooth. For a long-lived resonance, that is, when $\Gamma(R, R'; E)$ is much smaller than the period of vibration, the cross sections consist of a series of peaks reflecting the vibrational states of the resonant state. This dependence of the cross section on the lifetime of the resonance is illustrated in Fig. 9.10.

When the energy exceeds the dissociation energy, *dissociation* may occur, either indirectly through the resonant state, or directly through a transition to the continuum of the nuclear motion of the molecule. The indirect process contributes only when the target is initially in a high excited vibrational state (45). Usually, the direct process dominates. For large enough energies, the adiabatic approximation applies and the dissociation cross section is given by

$$d\sigma^{\rm D}_{\nu_i\to\omega_f} = \frac{(2\pi)^4}{k_i}|T_{\omega_f\nu_i}(\Omega_f, \Omega_i)|^2 d\Omega_f \tag{9.46}$$

with

$$T_{\omega_f\nu_i}(\Omega_f, \Omega_i) = \int dR F^*_{\omega_f}(R) t(\Omega_f, \Omega_i, R) F_{\nu_i}(R) \ , \tag{9.47}$$

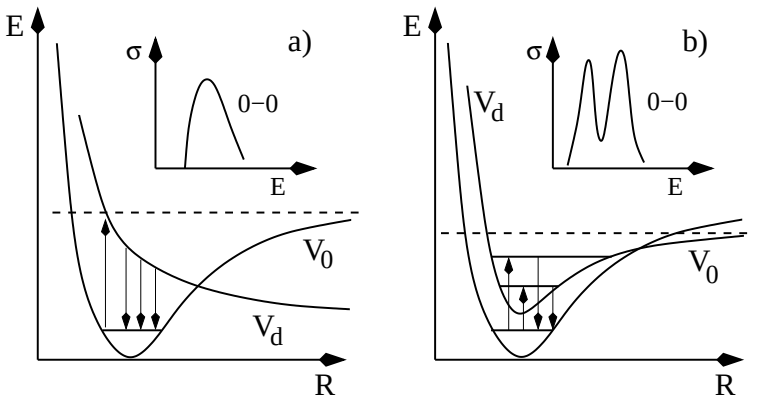

Figure 9.10: Illustration of resonant vibrational excitation of a molecule for a large (a) and a small (b) imaginary part of $F(R, R'; E)$. The dashed line indicates the dissociation threshold, $V_0(R)$ is the potential energy surface for the molecule, $V_d(R)$ is the potential energy surface for the auto-detaching resonant state of the negatively charged molecule, and the insets show the typical shape of the cross section for the two cases.

where $t(\Omega_f, \Omega_i, R)$ is the electronically elastic fixed-nuclei scattering amplitude and $F_{\omega_f}(R)$ is a continuum nuclear wavefunction of the molecule. Electronic quantum numbers are suppressed because they are unchanged; vibrational excitation and dissociation involve only one potential energy surface of the target molecule.

Finally, the *production of electronically excited molecules* occurs due to scattering with high energy electrons. For energies far away from the dissociation threshold, the adiabatic approximation holds. Therefore, ignoring the rotational degrees of freedom, the transition amplitude can be written as

$$\begin{aligned} T_{n_f\nu_f n_i\nu_i}(\Omega_f, \Omega_i) &= \int dR F^*_{n_f\nu_f}(R) t_{n_f n_i}(\Omega_f, \Omega_i, R) F_{n_i\nu_i}(R) \\ &= t_{n_f n_i}(\Omega_f, \Omega_i, R_0) \int dR F^*_{n_f\nu_f}(R) F_{n_i\nu_i}(R) \ . \end{aligned} \tag{9.48}$$

In the second line the fact has been utilized that $F_{n_i\nu_i}(R)$ is strongly peaked at $R = R_0$, where R_0 is the position of the minimum of the potential energy surface of the initial electronic state of the molecule. The differential cross section for electronic excitation is thus given by

$$d\sigma^{\rm EE}_{n_i\nu_i\to n_f\nu_f} = \frac{d\sigma^{R_0}_{n_i\to n_f}}{d\Omega_f} \left| \int dR F^*_{n_f\nu_f}(R) F_{n_i\nu_i}(R) \right|^2 d\Omega_f \ , \tag{9.49}$$

where the first factor is the fixed-nuclei differential cross section at $R = R_0$ for the electronic transition $n_i \to n_f$ and the second is the Franck-Condon factor q already mentioned in connection with ion-ion annihilation.

9.2.3 Concluding remarks

This section discussed elementary collision processes, as they typically occur in molecular gas discharges, focusing, in particular, on inelastic and reactive collisions which change the internal energy and composition of the scattering fragments: ionization, attachment, recombination, annihilation, detachment, and excitation. These processes are the primary driving force of the plasma-chemistry in these discharges. Elastic scattering, on the other hand, is not explicitly discussed, because its main effect, depositing energy into the electronic subsystem, affects the plasma-chemistry only indirectly.

Instead of merely listing kitchen-made cross section formulae and unrelated cross section data, emphasis has been given on an unified description of elementary processes based on general principles of quantum-mechanical multi-channel scattering theory. By necessity, the presentation is rather dense. Technical details left out, as well as cross section data, can be found, respectively, in the original papers and the review articles, monographs, and web-sites mentioned in the introduction.

As far as the kinetic modeling of gas discharges is concerned, collision cross sections are input parameters for the collision integrals of the Boltzmann equations. They are thus always convoluted with distribution functions. Some of the quantum-mechanical intricacies of particle en- and de-tanglement occurring during a collision are thus eventually averaged out. Calculating cross sections earmarked for plasma-chemical applications with the most sophisticated quantum-mechanical methods is thus not only not feasible for the (poly-atomic) gases of interest, it would be also overkill. Cross sections obtained from effective (semi-empirical) models containing only those microscopic degrees of freedom which, for given external control parameters, may eventually become active in the collision integrals, should be in fact sufficient. A systematic effort to develop (and solve) this type of models for the various processes may significantly increase the predictability of plasma modeling. It may thus help to turn plasma processing as a whole from an art to a science (46).

References

[1] U. Fano, Phys. Rev. A **24** (1981) 2402.

[2] M. J. Brunger, S. J. Buckman, Phys. Rep. **357** (2002) 215.

[3] L. G. Christophorou, J. K. Olthoff, Fundamental electron interactions with plasma processing gases (Kluwer Academic/Plenum Publishers, New York) (2004).

[4] W. L. Morgan, In M. Inokuti, K. H. Becker, editors, Advances in atomic, molecular, and optical physics, volume 43 (Academic Press, San Diego) (2000), 79.

[5] P. G. Burke, J. Tennyson, Molecular Physics **103** (2005) 2537.

[6] C. Winstead, V. McKoy, Comp. Phys. Comm. **128** (2000) 386.

[7] H. Bethe, Ann. Phys. (Leipzig) **5** (1930) 325.

[8] L. Vriens, In E. W. McDaniel, M. R. C. McDowell, editors, Case studies in atomic physics, volume 1 (North-Holland, Amsterdam) (1969), 335.

[9] Y.-K. Kim, M. E. Rudd, Phys. Rev. A **50** (1994) 3954.

[10] H. Deutsch, K. Becker, S. Matt, T. D. Maerk, Int. J. Mass. Spectrometry **197** (2000) 37.

[11] H. Deutsch, P. Scheier, K. Becker, T. D. Maerk, Int. J. Mass. Spectrometry **233** (2004) 13.

[12] H. Deutsch, P. Scheier, S. Matt-Leubner, K. Becker, T. D. Maerk, Int. J. Mass. Spectrometry **243** (2005) 215.

[13] T. F. O'Malley, Phys. Rev. **150** (1966) 14.

[14] J. N. Bardsley, A. Herzenberg, F. Mandl, Proc. Phys. Soc. **89** (1966) 321.

[15] J. N. Bardsley, Proc. Phys. Soc. **91** (1967) 300.

[16] A. Herzenberg, Phys. Rev. **160** (1967) 80.

[17] J. N. Bardsley, J. Phys. B (Proc. Phys. Soc.) **1** (1968) 349.

[18] J. N. Bardsley, J. Phys. B (Proc. Phys. Soc.) **1** (1968) 365.

[19] L. Dube, A. Herzenberg, Phys. Rev. A **20** (1979) 194.

[20] R. E. Olson, J. Chem. Phys. **56** (1972) 2979.

[21] R. E. Olson, F. T. Smith, E. Bauer, Applied Optics **10** (1971) 1848.

[22] E. Gerjuoy, Annals of Physics **5** (1958) 58.

[23] R. G. Newton, Scattering theory of waves and particles (McGraw-Hill Book Company, New York) (1966).

[24] A. G. Sitenko, Scattering theory (Springer-Verlag, Berlin) (1991).

[25] M. R. H. Rudge, Rev. Mod. Phys. **40** (1968) 564.

[26] J. N. Bardsley, F. Mandl, Rep. Prog. Phys. **31** (1968) 471.

[27] M. Inokuti, Rev. Mod. Phys. **43** (1971) 297.

[28] N. F. Lane, Rev. Mod. Phys. **52** (1980) 29.

[29] J. B. Delos, Rev. Mod. Phys. **53** (1981) 287.

[30] A. Chutjian, A. Garscadden, J. M. Wadehra, Phys. Rep. **264** (1996) 393.

[31] Y. Hahn, Rep. Prog. Phys. **60** (1997) 691.

[32] A. I. Florescu-Mitchell, J. B. A. Mitchell, Phys. Rep. **430** (2006) 277.

[33] L. W. Boltzmann, Ber. Wien. Akad. **66** (1872) 275.

[34] J. Wilhelm, R. Winkler, Annalen der Physik (Leipzig). **36** (1979) 333.

[35] K. Matyash, R. Schneider, F. Taccogna, A. Hatayama, S. Longo, M. Capitelli, D. Tskhakaya, F. X. Bronold, Contr. Plasma Physics **8-9** (2007) 595.

[36] M. Shugard, A. U. Hazi, Phys. Rev. A **12** (1975) 1895.

[37] W. Domcke, Phys. Rep. **208** (1991) 97.

[38] H.-D. Meyer, Phys. Rev. A **40** (1989) 5605.

[39] J. Brand, L. S. Cederbaum, H.-D. Meyer, Phys. Rev. A **60** (1999) 2983.

[40] A. K. Kazansky, I. S. Yelets, J. Phys. B: At. Mol. Opt. Phys. **17** (1984) 4767.

[41] A. K. Kazansky, S. A. Kalin, J. Phys. B: At. Mol. Opt. Phys. **23** (1990) 809.

[42] S. A. Kalin, A. K. Kazansky, J. Phys. B: At. Mol. Opt. Phys. **23** (1990) 3017.

[43] A. Giusti, J. Phys. B: At. Mol. Phys. **13** (1980) 3867.

[44] S. A. Akhmanov, K. S. Klopovskii, A. P. Osipov, Sov. Phys. JETP **56** (1982) 936.

[45] D. E. Atems, J. M. Wadehra, J. Phys. B: At. Mol. Phys. **26** (1993) L759.

[46] A. Jacob, Solid State Technology **26** (1983) 151.